Multimedia operator chain topology and ordering estimation based on detection and information theoretic tools

Pedro Comesaña [#] and Fernando Pérez-González [#⋆⋆]

[#] Signal Theory and Communications Department, University Vigo
E. E. Telecomunicación, Campus-Lagoas Marcosende, Vigo 36310, Spain
[⋆] Gradiant (Galician Research and Development Center in
Advanced Telecommunications), Vigo 36310, Spain
{pcomesan,fperez}@gts.tsc.uvigo.es
http://www.gts.tsc.uvigo.es/gpsc/

Abstract. The extensive use of multimedia editing tools suitable for non-skilled users has significantly reduced the trust on audiovisual contents. Simultaneously, a new branch of multimedia security, named multimedia forensics, has been developed to cope with this problem. Nevertheless, most of the schemes proposed so far are heuristic and ad-hoc solutions that try to deal with a particular signal processing operator (or a simple combination of them). In a previous work by the authors, fundamental limits to forensics applications are provided, based on the use of two well-known measures, originated at the detection and information theory fields. In the current work the suitability of those measures for establishing the topology and ordering of the operator chain a multimedia content has gone through is illustrated. The provided results show that in general different operator chains can be distinguished, altough in some particular cases (e.g., comparison between double and triple quantization) the considered operator chains can be completely indistinguishable.

Keywords: Multimedia forensics, ordering detection, topology detection, operator parameter estimation.

1 Introduction

In the last decades the number of multimedia contents and their impact in our lives has dramatically increased. The cost reduction of capture devices, especially digital cameras, and the growth of digital networks where those contents can be

[⋆] Research supported by the European Union under project REWIND (Grant Agreement Number 268478), the European Regional Development Fund (ERDF) and the Spanish Government under projects DYNACS (TEC2010-21245-C02-02/TCM) and COMONSENS (CONSOLIDER-INGENIO 2010 CSD2008-00010), and the Galician Regional Government under projects "Consolidation of Research Units" 2009/62, 2010/85 and SCALLOPS (10PXIB322231PR).

published have converted multimedia contents not only in valuable proofs of our personal evolution and social life, but also in a weapon that can be used to harm the public image of individuals. Therefore, multimedia contents have evolved to be considered precious assets with both implicit and explicit value that one would like to preserve. However, together with this growth, a huge number of editing tools available in applications for non-skilled users have proliferated during this time, thus compromising the reliability of those contents, and strongly constraining their use in some applications, for example as court evidence. As a consequence, trust on multimedia contents has steadily decreased.

In this context, multimedia forensics, an area of multimedia security, has appeared as a possible solution to the decrease of confidence on multimedia contents. The target of multimedia forensics can be summarized as assessing the processing, coding and editing steps a content has gone through. Although much effort has been paid to this topic in the last years, most of the proposed solutions are somewhat heuristic ad-hoc methods that do not answer to the question of what is the optimal way of detecting the operators the contents have undergone, or how easily different operator chains can be distinguished. Answers to those fundamental questions are provided in a previous work by the authors [3], proposing the use of detection and information theoretic measures. The target of this work is to provide distinguishability results on a number of new scenarios not analyzed so far, as well as illustrating the suitability of those measures for identifying the operator chain ordering.

The remaining of this paper is organized as follows: previous approaches to multimedia forensics problems, paying special attention to JPEG and double JPEG quantization, are summarized in Sect. 2; the proposed measures are presented in Sect. 3. Sect. 4 presents some experimental results on three relevant practical scenarios, while Sect. 5 reports results on the use of those measures for distinguishing the ordering of operators in processing chains. Finally, Sect. 6 summarizes the main conclusions of this work and discusses future lines.

2 Previous works on quantization and double quantization detection and estimation

In this section we give a brief overview of some state-of-the-art forensics methods dealing with quantization; our interest in that operator is related to the scenarios analyzed in Sect. 4, which in turn are just an example of the applicability of the measures we propose to use in forensics. By no means we try to be exhaustive, but simply provide a rough picture of some of the solutions that have been proposed in the last years, emphasizing their ad-hoc and/or heuristic nature.

One of the first works in the literature dealing with the single quantization detection and estimation is due to Fan and Queiroz [5], where the detection statistic depends on the difference between the histogram of the pixel differences across blocks and within blocks. Once the quantization is detected, a Maximum Likelihood (ML) estimator, based on assuming that the AC DCT coefficients follow a Laplacian distribution, is used for estimating the quantization step. A

completely different approach was proposed by Lin *et al.* in [7], where in order to check the suitability of a candidate transform, the authors try to estimate the pdf of the original (unquantized) coefficients by interpolating the histogram of the observed coefficients, and then compute the normalized correlation between this pdf approximation and the observed histogram; if the obtained value is high, then the considered transform will likely be the one used in coding. In another relevant work [10], the variability of the integral of the AC DCT coefficients in different intervals is exploited in order to detect the quantization artifacts; the same idea is then used to determine the transform encoder.

Concerning double quantization, in [8] Lukas and Fridrich propose a method for estimating the first quantization matrix; they study some characteristic features that appear in DCT coefficient histograms when those coefficients are quantized; although several strategies are proposed, the most successful one is based on neural networks. An alternative approach is proposed by Fu *et al.* in [6], where a generalized version of Benford's law is exploited for JPEG detection and estimation, and double JPEG detection. In [11], Milani *et al.* also exploit the distribution of the most significant digits of DCT coefficients, modeled according to Benford's law, to estimate the number of compression stages the image has gone through. In another proposal, Luo *et al.* [9] study the blocking artifacts introduced by misaligned double JPEG coding; with the help of a SVM that information is used to determine if an image is a JPEG original or it was cropped from other JPEG image and re-saved as JPEG. The non-aligned double JPEG artifacts on the pdf of the DCT coefficients are exploited in [1] for locating image forgeries.

3 Distinguishability measures

This section summarizes the reasons for using the distinguishability measures exploited in Sects. 4 and 5. Since an extensive motivation of their use was already provided in [3], the current work will just recall their advantages and definitions (the interested reader is referred to [3]).

First of all, the desirable characterisitcs of our distinguishability measures are enumerated:

- they should be capable of reliably determining if a multimedia content has gone through an arbitrary chain of operators which are arranged in a particular ordering and topology.
- they should allow to quantify how easily two different chains of operators (characterized by their ordering and topology, and where in some circumstances additional knowledge on the operator parameters is assumed) can be distinguished.
- some optimality criterion should be followed; for example, minimizing the false positive probability (i.e., determining that the considered content has gone through a given operator chain, when it has not) for a given false negative probability (i.e., saying that the content has not undergone a given operator chain, when indeed it has).

– it is also desirable the detection scheme to be blind, meaning that deterministic knowledge of the original multimedia content should not be required, although some kind of *a priori* information about the original statistical distribution will typically be assumed to be known.

Based on these requirements, the use of two different measures is proposed for distinguishing operator chains.

3.1 Detection-theoretic measure

From a detection theory point of view the problem of determining which distribution out of two possible candidates produced a given observation, is modeled as a binary hypothesis test; it is well known that the most powerful test (i.e., that one minimizing the probability of false positive for a given false negative probability) in that scenario is given by the Neyman-Pearson Lemma, which uses the likelihood-ratio between the so-called null hypothesis (denoted by θ_0) and the alternative hypothesis (denoted by θ_1), i.e., $\Lambda(\mathbf{x}) = \frac{p(\theta_0|\mathbf{x})}{p(\theta_1|\mathbf{x})}$, where $\mathbf{x}$ denotes the n-dimensional signal under test. Assuming that no *a priori* information about the different hypotheses is available, the former ratio is equivalent to

$$\mathrm{LLR}(\mathbf{x}) = \log\left(\frac{p(\mathbf{x}|\theta_0)}{p(\mathbf{x}|\theta_1)}\right),$$

for the discrete case (the continuous counterpart has an analogous form). For the sake of notational simplicity we will use $p(\mathbf{x}|\theta_i) = p_i(\mathbf{x})$.

Be aware that θ_0 and θ_1 define the considered operator chain topology (i.e., how the operators are linked, in parallel or series) and ordering, as well as the specific parameters characterizing each operator. Therefore, the generality objective is achieved by this measure, as it can be useful, among others, for detecting:

– the ordering and topology of the operator chain whenever a fixed set of operators, each of them using fixed parameters, is considered;
– the presence of different operators in chains sharing the same topology;
– the use of different operator parameters in processing chains using the same operators with common ordering and topology;
– combinations of the previous scenarios.

3.2 Information-theoretic measure

Concerning information-theoretic measures devoted to quantify the differences between two pdfs/pmfs, probably the most used choice is the Kullback-Leibler divergence (a.k.a. Kullback-Leibler distance and relative entropy). This measure was used, for example, for quantifying the statistic detectability of the watermark embedding in steganography [2]. For the discrete case it is defined as

$$D(p_0||p_1) = \sum_{\mathbf{x}\in\mathcal{X}} p_0(\mathbf{x}) \log\left(\frac{p_0(\mathbf{x})}{p_1(\mathbf{x})}\right),$$

where $\mathcal{X}$ is the discret alphabet where $\mathbf{x}$ takes values. The KLD is non-negative, being null if and only if the two considered distributions are the same almost everywhere; indeed, in order to provide an intuitive insight, one can say that the closer two distributions are, the smaller their KLD is.

Concerning the relationship between both measures, it is a well-known result that the relative entropy version of the Asymptotic Equipartition Property establishes that if $\mathbf{X}$ is a sequence of random variables drawn i.i.d. according to $p_0(\mathbf{x})$, then $\frac{1}{n}\log\left(\frac{p_0(\mathbf{X})}{p_1(\mathbf{X})}\right) \rightarrow D(p_0||p_1)$, where convergence takes place in probability [4]. In plain words, this result shows that when the contents produced under the null hypothesis are i.i.d. and the dimensionality of the considered problem goes to infinity, then the two measures whose use is proposed for forensic applications are asymptotically equivalent. This confirms that both measures are good candidates for quantifying the distinguishability between different operator chain topologies, and/or operator chains with different operator parameters, providing a coherent framework.

Finally, the Chernoff-Stein Lemma [4] states that the false positive probability error exponent achievable for a given non-null false negative probability asymptotically converges to $D(p_0||p_1)$ (as long as that measure takes a finite value) when the dimensionality of the problem goes to infinity.

4 Studied scenarios

In this section the mentioned distinguishability measures are used for quantifying the closeness between the distributions corresponding to different operator parameters of three operator chains, i.e., for quantifying how easily the use of different processing parameters in those operator chains could be identified. The operator parameters used for generating the considered samples (i.e., those corresponding to the null hypothesis) will be denoted by the subindex 0, while 1 will refer to the tested values (corresponding to the alternative hypothesis). In case that a subindex were already used for denoting the corresponding parameter (e.g., Δ_i), a second subindex will be added for denoting the null or alternative hypothesis (i.e., $\Delta_{i,j}$, where $j = 0, 1$).

The used distinguishability measures will be those introduced in Sect. 3, i.e., the LLR of the observed signal for the null and alternative hypotheses, and the KLD; in the latter case two choices are considered for the null hypothesis distribution: the theoretical distribution, and its empirical counterpart, i.e., the histogram of the considered content.

4.1 Scenario 1: Quantization; Gamma correction; Quantization

– **Operator chain description**: the input content (e.g., an image) is quantized (with quantization stepsize Δ_1), for example due to Analog to Digital Conversion. Then, the obtained digital content goes through gamma correction with parameter γ in order to improve the contrast; as the levels of the output signal do not belong to a lattice (i.e., they are not equidistant), a second quantization

(with quantization stepsize Δ_2) is performed in order to produce a content with equidistant coding levels. The last quantization stepsize is assumed to be known.

- **Application scenario**: an image is captured using a lossless format (such as TIFF), and then it is gamma-corrected to improve its contrast; as the output of the corrector is in general a real number, a second quantization must be performed in order to produce an output TIFF image. In this example of use, compression algorithms (e.g., JPEG) are not considered, as the quantization and the gamma correction should be performed in the same domain; given that the gamma correction is usually applied in the pixel domain, that should be also the case for the quantization, while those compression algorithms most of times work in a transform domain (as the DCT). Since the considered processing operates pointwise, the dependence among neighboring pixels of natural images can be neglected for our analysis. Although an accurate pdf model would probably require a more complicated characterization, since these scenarios just try to illustrate the usefulness of the proposed measures, we will model the pixels by an i.i.d. Gaussian with mean $\mu_X = 128$ and variance $\sigma_X^2 = 240$, truncated to lie in the interval $[0, 255]$.
- **PMF theoretical model**: in this case it will be useful to introduce the pmf of the signal at the output of the first quantizer, which is given by

$$p^{\text{quant}_1}(k\Delta_1|\Delta_1) = \begin{cases} \mathcal{Q}\left(\frac{k\Delta_1-\Delta_1/2-\mu_X}{\sigma_X}\right) - \mathcal{Q}\left(\frac{k\Delta_1+\Delta_1/2-\mu_X}{\sigma_X}\right), & \text{if } k \in \mathbb{N},\ k > 0,\ \text{and } k < \left(\frac{255}{\Delta_1} - \frac{1}{2}\right) \\ 1 - \mathcal{Q}\left(\frac{\Delta_1/2-\mu_X}{\sigma_X}\right), & \text{if } k = 0 \\ \mathcal{Q}\left(\frac{k_1\Delta_1-\Delta_1/2-\mu_X}{\sigma_X}\right), & \text{if } k = k_1 \\ 0, & \text{otherwise} \end{cases},$$

where $k_1 = \lceil \frac{255}{\Delta_1} - \frac{1}{2} \rceil$, and $\mathcal{Q}(x) = \int_x^\infty \frac{e^{\frac{-\tau^2}{2}}}{\sqrt{2\pi}} d\tau$. Based on this distribution, the pmf of the operator chain output in this scenario is given by

$$p^1(k\Delta_2|\Delta_1, \gamma, \Delta_2) = \sum_{m \in \mathcal{M}_k} p^{\text{quant}_1}(m\Delta_1|\Delta_1),$$

where $\mathcal{M}_k = \left\{ m : Q_{\Delta_2}\left(255\left[\frac{m\Delta_1}{255}\right]^\gamma\right) = k\Delta_2 \right\}$, $Q_\Delta(\cdot)$ is the uniform scalar quantizer with stepsize Δ.

- **Known/unknown parameters**: the first quantization stepsize will be denoted by Δ_1, and the gamma correction parameter by γ; both are assumed to be unknown to the forensics analyst. On the other hand, the second quantization stepsize Δ_2, as well as the mean and variance of the input signal will be assumed to be known.
- **Results**: Figs. 1, and 2 show the theoretical and empirical KLDs, as well as the LLR for $\Delta_{1,0} = 1$ (first quantization stepsize for the null hypothesis), $\gamma_0 = 0.9$ (gamma correction factor for the null hypothesis), $\Delta_{2,0} = \Delta_{2,1} = 4$ (the second quantization stepsize used for producing the input content is assumed to be known, as it can be easily estimated by the forensics analyst), and $n = 10^6$. As one would expect, the minimum of the considered functions are located at $\Delta_{1,1} = 1$ and $\gamma_1 = 0.9$, showing that for this case, the two hypotheses would be least distinguishable.

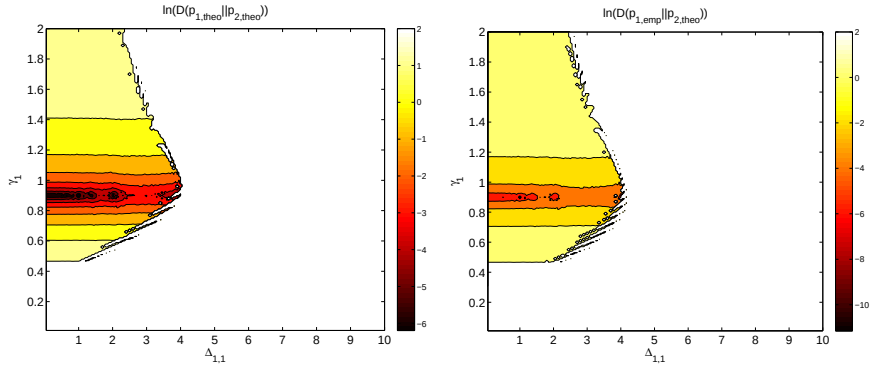

Fig. 1. Theoretical (a) and empirical (b) KLD for Scenario 1. $\Delta_{1,0} = 1$, $\gamma_0 = 0.9$, $\Delta_{2,0} = \Delta_{2,1} = 4$, $n = 10^6$.

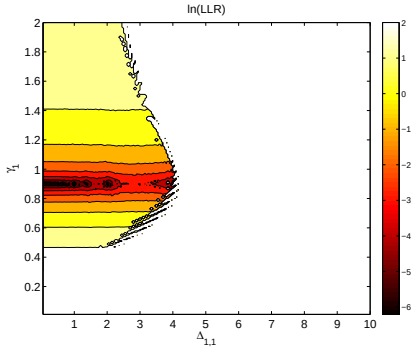

Fig. 2. LLR for Scenario 1. $\Delta_{1,0} = 1$, $\gamma_0 = 0.9$, $\Delta_{2,0} = \Delta_{2,1} = 4$, $n = 10^6$.

4.2 Scenario 2: Gamma correction; Quantization; Quantization

- **Operator chain description**: this scenario is very similar to the previous one, but in this case the first quantization and the gamma correction are swapped. The relevance of considering these two related scenarios is that later we will show that the proposed measures are able to distinguished between them, illustrating their ability for determining operator ordering, even when the parameters used in those operators are not known by the forensics analyst.
- **Application scenario**: an example of use of this scenario is a framework where we have a camera with an analog gamma corrector; then, the corrected analog signal is digitized (so a first fine quantization must be considered). Finally, trying to fool the forensics analyst, or just in order to reduce the size of the produced image, a second quantizer is used (e.g., the original signal could use 12 bits for

coding each color component of a pixel, while the output of the second quantizer could use just 8).

– **PMF theoretical model**: in this case the pmf of the signal at the output of the first quantizer is

$$p^{\text{quant}_2}(k\Delta_1|\Delta_1) = \begin{cases} \mathcal{Q}\left(\frac{255\left(\frac{k\Delta_1-\Delta_1/2}{255}\right)^{1/\gamma}-\mu_X}{\sigma_X}\right) - \mathcal{Q}\left(\frac{255\left(\frac{k\Delta_1+\Delta_1/2}{255}\right)^{1/\gamma}-\mu_X}{\sigma_X}\right), & \text{if } k \in \mathbb{N},\, k>0, \\ & \text{and } k < \left(\frac{255}{\Delta_1}-\frac{1}{2}\right) \\ 1-\mathcal{Q}\left(\frac{255\left(\frac{\Delta_1/2}{255}\right)^{1/\gamma}-\mu_X}{\sigma_X}\right), & \text{if } k=0 \\ \mathcal{Q}\left(\frac{255\left(\frac{k_2\Delta_1-\Delta_1/2}{255}\right)^{1/\gamma}-\mu_X}{\sigma_X}\right), & \text{if } k=k_2 \\ 0, & \text{otherwise} \end{cases},$$

where $k_2 = \lceil \frac{255}{\Delta_1} - \frac{1}{2} \rceil$. Based on this distribution, the pmf on this scenario is given by

$$p^2(k\Delta_2|\gamma,\Delta_1,\Delta_2) = \sum_{m\in\mathcal{L}_k} p^{\text{quant}_2}(m\Delta_1|\Delta_1),$$

where $\mathcal{L}_k : \{m : Q_{\Delta_2}(m\Delta_1) = k\Delta_2\}$.

– **Known/unknown parameters**: similarly to the previous case, the gamma correction parameter γ, and the first quantization stepsize Δ_1 will be assumed to be unknown to the forensics analyst. On the other hand, the second quantization stepsize Δ_2, as well as the mean and variance of the input signal will be assumed to be known.

– **Results**: Figs. 3, and 4 show the theoretical and empirical KLDs, as well as the LLR for $\gamma_0 = 0.9$ (gamma correction factor under the null hypothesis), $\Delta_{1,0} = 1$ (first quantizer stepsize for the null hypothesis), $\Delta_{2,0} = \Delta_{2,1} = 4$ (second quantizer stepsizes for the null and alternative hypothesis, respectively), and $n = 10^6$. Again, as one would expect the minima of the considered functions are located at $\gamma_1 = 0.9$ and $\Delta_{1,1} = 1$. It is interesting to note that values of γ_1 even slightly smaller than γ_0 produce very large values of the considered target functions. Finally, one can observe that the cases where $\Delta_{1,1} > \Delta_{2,0}$ are easily discarded; this is due to the presence of centroids with non-null probability that will not be feasible under the alternative hypothesis.

4.3 Scenario 3: Filtered white Gaussian signal with channel $\mathbf{h} = (1, h(1), h(2))$

– **Operator chain description**: this scenario considers the effect of filtering white Gaussian signal (with mean $\mu_X = 0$) with an FIR filter of order 2. This example must be regarded as a very simple case of filtering detection and estimation, where those tasks are assisted by the knowledge of the input distribution to the filter. Additionally to its inherent interest, we think that the study of this framework is also worthy due to the addition of memory.

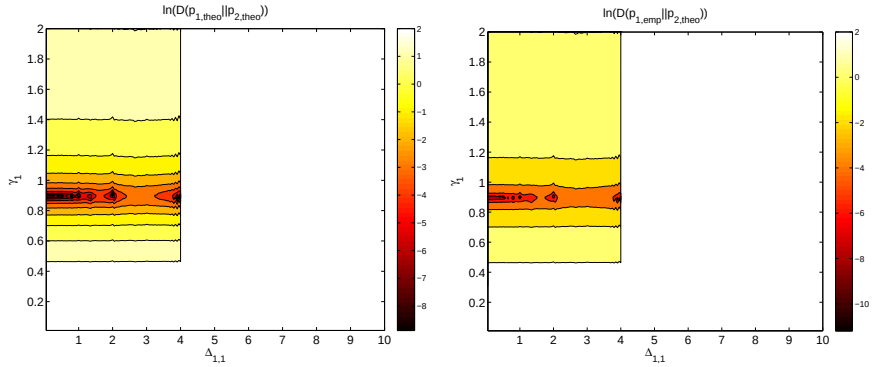

Fig. 3. Theoretical (a) and empirical (b) KLDs for Scenario 2. $\gamma_0 = 0.9$, $\Delta_{1,0} = 1$, $\Delta_{2,0} = \Delta_{2,1} = 4$, $n = 10^6$.

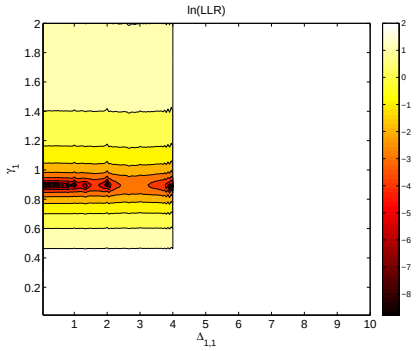

Fig. 4. LLR for Scenario 2. $\gamma_0 = 0.9$, $\Delta_{1,0} = 1$, $\Delta_{2,0} = \Delta_{2,1} = 4$, $n = 10^6$.

– **Application scenario**: this scenario must be regarded as a filtering toy example, showing the power of the proposed measures for dealing with systems with memory. Indeed, due to the memory constraint and the subsequent correlation between vector components, if one wants to obtain the empirical results in this scenario by using the histogram, as we did in the previous sections, then and n-dimensional histogram should be considered; nevertheless, for large values of n one would expect the output signal to be sparsely distributed in that n-dimensional space, and consequently the histogram computation would not be feasible for a realistic number of observed n-dimensional vectors. Therefore, in this scenario a parameterized estimation is followed; specifically, the observed samples are used for estimating by ML the corresponding Gaussian pdfs, parameterized by the sample mean (assumed to be the same for each sample) and covariance matrix (with size $n \times n$). A set of L n-dimensional filtered vectors

(i.e., vectors at the output of the filter under analysis) will be considered in this estimation.

– **PDF theoretical model**: in this case it is well known that

$$f^3(\mathbf{x}|\mu_Y, \Sigma) = \frac{e^{-\frac{1}{2}(\mathbf{x}-\mu_Y)^T \Sigma^{-1}(\mathbf{x}-\mu_Y)}}{(2\pi)^{n/2} |\Sigma|^{1/2}}, \tag{1}$$

where μ_Y is the mean of the filtered content (so if we are computing the theoretical pdf, based on $\mu_X = 0$, it is evident that $\mu_Y = 0$) and Σ is the covariance matrix, which for the theoretical pdf, assuming that $\mathbf{h} = (1, h(1), h(2))$ is used, will be the result of substracting to the symmetric Toeplitz matrix with main diagonal elements equal to $1 + h(1)^2 + h(2)^2$, first diagonal elements equal to $[1 + h(2)]h(1)$, and second diagonal elements $h(2)$ (all the remaining elements being null), the matrix whose element at position $(1, 1)$ is $h(1)^2 + h(2)^2$, that at position $(2, 2)$ is $h(2)^2$, and those at $(2, 1)$ and $(1, 2)$ are $h(2)h(1)$ (i.e., the steady regime covariance matrix, minus the disturbances from the Toeplitz structure due to the filter boundary effect).
On the other hand, in this scenario the use of the histogram for dealing with the empirical pdf would be impractical. Instead, the ML estimation of the mean and covariance matrix will be performed; the estimates will be replaced in (1).

– **Known/unknown parameters**: for the sake of simplicity we will assume that $h(0) = 1$. The other two coefficients of the filter will be assumed to be unknown by the forensics analyst.

– **Results**: Figs. 5, and 6 show the theoretical and empirical KLDs, and the LLR for the considered scenario. The filter used under the null hypothesis is $\mathbf{h}_0 = (1, 0.4, -0.2)$, and $\sigma_X^2 = 2$. It is worth highlighting the almost triangular shape of the level curves for all the 3 proposed measures; this fact can be shown to be related to the stability triangle of $\mathbf{h}_0$.

5 Distinguishing operator chain topologies

In the scenarios studied in the previous section we have checked the distinguishability capabilities of the proposed measures when the same operators in the same ordering and topology are compared, i.e., we were just analyzing how easily the impact of the same operator chain could be distinguished for different operator parameters. Indeed, in all the scenarios considered so far the null hypothesis belongs to the alternative hypothesis search space, so there was at least a point, where the parameters corresponding to the alternative hypothesis are equal to those corresponding to the null hypothesis, that yields a null value of the KLD between the theoretical pmf corresponding to the null hypothesis and its alternative hypothesis counterpart, as well as a null value of the LLR.

In the last two scenarios this framework will be changed. First, we will compare two pairs of the operator chains using the same elementary operator but a different number of times; namely, double vs. triple quantization. Then, we will

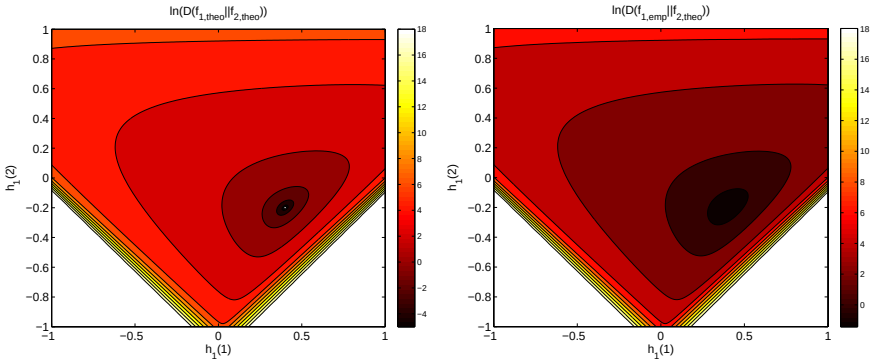

Fig. 5. Theoretical (a) and empirical (b) KLD for Scenario 3. $\mathbf{h}_0 = (1, 0.4, -0.2)$, $n = 10^4$, $L = 10^2$, $\sigma_X^2 = 2$.

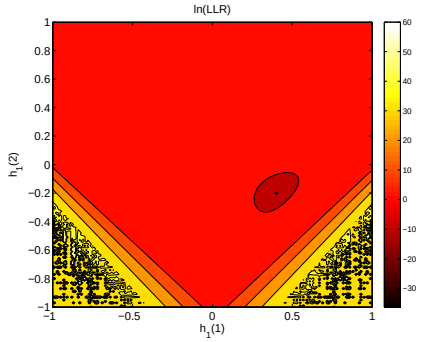

Fig. 6. LLR for Scenario 3. $\mathbf{h}_0 = (1, 0.4, -0.2)$, $n = 10^4$, $L = 10^2$, $\sigma_X^2 = 2$.

focus on the study of ordering, analyzing two different operator chains composed by the same elementary operators.

The comparison measures used here will be based on those described in Sect. 3; specifically, since we are interested in determining which is the closest alternative distribution to the null distribution, the proposed comparison measures are

$$\min_{\psi_1 \in \Psi_1} D(f(\mathbf{x}|\psi_0)||f(\mathbf{x}|\psi_1)), \quad \text{and} \quad \min_{\psi_1 \in \Psi_1} \log\left(\frac{f(\mathbf{X}|\psi_0)}{f(\mathbf{X}|\psi_1)}\right),$$

Ψ_1 is the set of values where the alternative hypothesis operator parameters are searched for. A detailed motivation of these measures can be found in [3].

5.1 Scenario 4: Double quantization vs. triple quantization

In this section the pdfs and samples produced by using 2 and 3 serially concatenated quantizers are compared. The detailed analysis of each those operator chains can be found in [3]; similarly to there, we will model original signal coefficients in the DCT domain by a Laplacian distribution. Denoting by $p^{\text{theo},k\text{-q}}$ the theoretical pmf when k quantizers are considered, and by $p^{\text{emp},k\text{-q}}$ the corresponding histogram, the obtained results for $n = 10^6$ are the following

$$\min_{(\Delta_{1,1},\Delta_{2,1})\in\mathbb{R}^+\times\mathbb{R}^+} D(p^{\text{theo,2-q}}(\mathbf{x}|\Delta_{1,0}=5,\Delta_{2,0}=9)||p^{\text{theo,3-q}}(\mathbf{x}|\Delta_{1,1},\Delta_{2,1},\Delta_{3,1}=9))=0,$$

$$\min_{(\Delta_{1,1},\Delta_{2,1})\in\mathbb{R}^+\times\mathbb{R}^+} D(p^{\text{emp,2-q}}(\mathbf{x}|\Delta_{1,0}=5,\Delta_{2,0}=9)||p^{\text{theo,3-q}}(\mathbf{x}|\Delta_{1,1},\Delta_{2,1},\Delta_{3,1}=9))=1.5\cdot 10^{-5},$$

$$\min_{(\Delta_{1,1},\Delta_{2,1})\in\mathbb{R}^+\times\mathbb{R}^+} \log\left(\frac{p^{\text{theo,2-q}}(\mathbf{x}|\Delta_{1,0}=5,\Delta_{2,0}=9)}{p^{\text{theo,3-q}}(\mathbf{x}|\Delta_{1,1},\Delta_{2,1},\Delta_{3,1}=9)}\right)=0,$$

$$\min_{\Delta_{1,1}\in\mathbb{R}^+} D(p^{\text{theo,3-q}}(\mathbf{x}|\Delta_{1,0}=4,\Delta_{2,0}=7,\Delta_{3,0}=9)||p^{\text{theo,2-q}}(\mathbf{x}|\Delta_{1,1},\Delta_{2,1}=9))=0.0438,$$

$$\min_{\Delta_{1,1}\in\mathbb{R}^+} D(p^{\text{emp,3-q}}(\mathbf{x}|\Delta_{1,0}=4,\Delta_{2,0}=7,\Delta_{3,0}=9)||p^{\text{theo,2-q}}(\mathbf{x}|\Delta_{1,1},\Delta_{2,1}=9))=0.0435,$$

$$\min_{\Delta_{1,1}\in\mathbb{R}^+} \log\left(\frac{p^{\text{theo,3-q}}(\mathbf{x}|\Delta_{1,0}=4,\Delta_{2,0}=7,\Delta_{3,0}=9)}{p^{\text{theo,2-q}}(\mathbf{x}|\Delta_{1,1},\Delta_{2,1}=9)}\right)=0.0435,$$

while when the same operator chain topology and ordering is considered

$$\min_{\Delta_{1,1}\in\mathbb{R}^+} D(p^{\text{theo,2-q}}(\mathbf{x}|\Delta_{1,0}=5,\Delta_{2,0}=9)||p^{\text{theo,2-q}}(\mathbf{x}|\Delta_{1,1},\Delta_{2,1}=9))=0,$$

$$\min_{\Delta_{1,1}\in\mathbb{R}^+} D(p^{\text{emp,2-q}}(\mathbf{x}|\Delta_{1,0}=5,\Delta_{2,0}=9)||p^{\text{theo,2-q}}(\mathbf{x}|\Delta_{1,1},\Delta_{2,1}=9))=2.1\cdot 10^{-5},$$

$$\min_{\Delta_{1,1}\in\mathbb{R}^+} \log\left(\frac{p^{\text{theo,2-q}}(\mathbf{x}|\Delta_{1,0}=5,\Delta_{2,0}=9)}{p^{\text{theo,2-q}}(\mathbf{x}|\Delta_{1,1},\Delta_{2,1}=9)}\right)=0,$$

$$\min_{(\Delta_{1,1},\Delta_{2,1})\in(\mathbb{R}^+)^2} D(p^{\text{theo,3-q}}(\mathbf{x}|\Delta_{1,0}=4,\Delta_{2,0}=7,\Delta_{3,0}=9)||p^{\text{theo,3-q}}(\mathbf{x}|\Delta_{1,1},\Delta_{2,1},\Delta_{3,1}=9))=0,$$

$$\min_{(\Delta_{1,1},\Delta_{2,1})\in(\mathbb{R}^+)^2} D(p^{\text{emp,3-q}}(\mathbf{x}|\Delta_{1,0}=4,\Delta_{2,0}=7,\Delta_{3,0}=9)||p^{\text{theo,3-q}}(\mathbf{x}|\Delta_{1,1},\Delta_{2,1},\Delta_{3,1}=9))=1.5\cdot 10^{-5},$$

$$\min_{(\Delta_{1,1},\Delta_{2,1})\in\mathbb{R}^+\times\mathbb{R}^+} \log\left(\frac{p^{\text{theo,3-q}}(\mathbf{x}|\Delta_{1,0}=4,\Delta_{2,0}=7,\Delta_{3,0}=9)}{p^{\text{theo,3-q}}(\mathbf{x}|\Delta_{1,1},\Delta_{2,1},\Delta_{3,1}=9)}\right)=0.$$

It is interesting to note that whenever the 2 quantizers scenario is considered as null hypothesis and the 3 quantizers scenario is the alternative hypothesis, the obtained results indicate that both scenarios cannot be distinguished. This result, although probably a bit surprising at first sight, can be easily explained; it means that whenever 3 quantizers are considered for the alternative hypothesis, one can find quantization stepsizes for the first and second quantizers such that the output of the total system is equivalent to that produced by just those two quantizers (the null hypothesis). In other words, there is at least one subcase within the alternative hypothesis search space that yields the same results that the null scenario. Indeed, in the considered framework several of those cases exist; just for the sake of illustration, we will enumerate some of them:

- $(\Delta_{1,1}, \Delta_{2,1}) = (5, 5)$: due to the idempotence of the two first quantizers, the cascade of the three quantizers in the alternative hypothesis is equivalent to the cascade considered by the null hypothesis.
- $(\Delta_{1,1}, \Delta_{2,1}) = (5, 9)$: one can follow a reasoning similar to the previous point, but considering in this case the last two quantizers.
- $(\Delta_{1,1}, \Delta_{2,1}) = (5/(2k+1), 5)$, where k is any non-negative integer value: the output of the second quantizer is the same that if one had $(\Delta_{1,1}, \Delta_{2,1}) = (5, 5)$, as the quantization region boundaries corresponding to $\Delta = 5$ are a subset of those corresponding to $\Delta = \frac{5}{2k+1}$.
- $(\Delta_{1,1}, \Delta_{2,1}) = (5, 9/(2k+1))$, with k any non-negative integer number: following a reasoning similar to the previous case, but considering the relationship between the quantization regions corresponding to the second and third quantizers.
- $(\Delta_{1,1}, \Delta_{2,1}) = (5, 5/k)$, where k is any positive integer number: if that relationship between the quantization stepsizes holds, then the second quantizer does not modify the quantized values, and consequently the same values will be obtained at the output of the third quantizer.
- $(\Delta_{1,1}, \Delta_{2,1}) = (5, \xi)$, where $0 < \xi < 1$: since the minimum distance between the points in $5\mathbb{Z}$ and $9\mathbb{Z} + 4.5$ (the quantizaton boundaries of the third lattice) is 0.5, if the quantization distortion is smaller than 0.5, then a change in the chosen centroid of the third lattice is not possible. The mentioned constraint on the quantization distortion is verified if $\Delta_{2,1} < 1$.
- $(\Delta_{1,1}, \Delta_{2,1}) = (5, \Delta_2^*)$, where Δ_2^* is any positive real number verifying

$$\left\{ \forall k \in \mathbb{Z}, \exists (k_2, k_3) : k_2 = \text{round}\left(\frac{k_1 \Delta_1}{\Delta_2}\right), k_3 = \text{round}\left(\frac{k_2 \Delta_2}{\Delta_3}\right), k_3 = \text{round}\left(\frac{k_1 \Delta_1}{\Delta_3}\right) \right\}.$$

Be aware that no every $\Delta_2^* > 0$ is a feasible solution to the previous problem, as the two values assigned to k_3 should coincide. Intuitively, the last formula means that we can consider any value of $\Delta_{2,1}$, as long as the result of quantizing the output of the first quantizer ($k_1 \Delta_1$, for any integer k_1) with the third quantizer, is equivalent to quantizing it first with the second quantizer, and then with the third one. Note that this last bullet is not implied by the previous ones; for example, $\Delta_2^* = 1.2$ verifies this constraint, while it does not satisfy any of the previous conditions.

On the other hand, whenever the triple quantization scenario is considered as the null hypothesis (i.e., the content under test is produced by going through three quantizers), it is easily distinguished from the double quantization case.

Finally, we would like to emphasize that the values of $D(p^{\text{emp},k\text{-q}} || p^{\text{theo},k'\text{-q}})$ correspond to consider a particular sample ($n = 10^6$), changing for each realization; in any case, the obtained results were always in the same order of magnitude that the reported data.

5.2 Scenario 5: Gamma;Quantization;Quantization vs. Quantization;Gamma;Quantization

When dealing with the comparison between the operator chains described in Scenarios 1 and 2 one has to consider the swapping of the location of the first

quantizer and the gamma corrector. Denoting by $p^{\text{theo},i}$ the theoretical pmf for the ith scenario, and by $p^{\text{emp},i}$ the corresponding histogram, the obtained results are the following,

$$\min_{(\gamma_1,\Delta_{1,1})\in\mathbb{R}^+\times\mathbb{R}^+} D(p^{\text{theo},1}(\mathbf{x}|\Delta_{1,0}=1,\gamma_0=0.9,\Delta_{2,0}=4)||p^{\text{theo},2}(\mathbf{x}|\gamma_1,\Delta_{1,1},\Delta_{2,1}=4)) = 2.8\cdot 10^{-3},$$

$$\min_{(\gamma_1,\Delta_{1,1})\in\mathbb{R}^+\times\mathbb{R}^+} D(p^{\text{emp},1}(\mathbf{x}|\Delta_{1,0}=1,\gamma_0=0.9,\Delta_{2,0}=4)||p^{\text{theo},2}(\mathbf{x}|\gamma_1,\Delta_{1,1},\Delta_{2,1}=4)) = 2.9\cdot 10^{-3},$$

$$\min_{(\gamma_1,\Delta_{1,1})\in\mathbb{R}^+\times\mathbb{R}^+} \log\left(\frac{p^{\text{theo},1}(\mathbf{x}|\Delta_{1,0}=1,\gamma_0=0.9,\Delta_{2,0}=4)}{p^{\text{theo},2}(\mathbf{x}|\gamma_1,\Delta_{1,1},\Delta_{2,1}=4)}\right) = 2.8\cdot 10^{-3},$$

$$\min_{(\gamma_1,\Delta_{1,1})\in\mathbb{R}^+\times\mathbb{R}^+} D(p^{\text{theo},2}(\mathbf{x}|\gamma_0=0.9,\Delta_{1,0}=1,\Delta_{2,0}=4)||p^{\text{theo},1}(\mathbf{x}|\Delta_{1,1},\gamma_1,\Delta_{2,1}=4)) = 5.1\cdot 10^{-4},$$

$$\min_{(\gamma_1,\Delta_{1,1})\in\mathbb{R}^+\times\mathbb{R}^+} D(p^{\text{emp},2}(\mathbf{x}|\gamma_0=0.9,\Delta_{1,0}=1,\Delta_{2,0}=4)||p^{\text{theo},1}(\mathbf{x}|\Delta_{1,1},\gamma_1,\Delta_{2,1}=4)) = 5.2\cdot 10^{-4},$$

$$\min_{(\gamma_1,\Delta_{1,1})\in\mathbb{R}^+\times\mathbb{R}^+} \log\left(\frac{p^{\text{theo},2}(\mathbf{x}|\gamma_0=0.9,\Delta_{1,0}=1,\Delta_{2,0}=4)}{p^{\text{theo},1}(\mathbf{x}|\Delta_{1,1},\gamma_1,\Delta_{2,1}=4)}\right) = 4.9\cdot 10^{-4},$$

while when the null hypothesis belongs to the search space of the alternative hypothesis (i.e., the same operator chain topology and ordering is considered)

$$\min_{(\gamma_1,\Delta_{1,1})\in\mathbb{R}^+\times\mathbb{R}^+} D(p^{\text{theo},1}(\mathbf{x}|\Delta_{1,0}=1,\gamma_0=0.9,\Delta_{2,0}=4)||p^{\text{theo},1}(\mathbf{x}|\Delta_{1,1},\gamma_1,\Delta_{2,1}=4)) = 0,$$

$$\min_{(\gamma_1,\Delta_{1,1})\in\mathbb{R}^+\times\mathbb{R}^+} D(p^{\text{emp},1}(\mathbf{x}|\Delta_{1,0}=1,\gamma_0=0.9,\Delta_{2,0}=4)||p^{\text{theo},1}(\mathbf{x}|\Delta_{1,1},\gamma_1,\Delta_{2,1}=4)) = 1.44\cdot 10^{-5},$$

$$\min_{(\gamma_1,\Delta_{1,1})\in\mathbb{R}^+\times\mathbb{R}^+} \log\left(\frac{p^{\text{theo},1}(\mathbf{x}|\Delta_{1,0}=1,\gamma_0=0.9,\Delta_{2,0}=4)}{p^{\text{theo},1}(\mathbf{x}|\Delta_{1,1},\gamma_1,\Delta_{2,1}=4)}\right) = 0,$$

$$\min_{(\gamma_1,\Delta_{1,1})\in\mathbb{R}^+\times\mathbb{R}^+} D(p^{\text{theo},2}(\mathbf{x}|\gamma_0=0.9,\Delta_{1,0}=1,\Delta_{2,0}=4)||p^{\text{theo},2}(\mathbf{x}|\gamma_1,\Delta_{1,1},\Delta_{2,1}=4)) = 0,$$

$$\min_{(\gamma_1,\Delta_{1,1})\in\mathbb{R}^+\times\mathbb{R}^+} D(p^{\text{emp},2}(\mathbf{x}|\gamma_0=0.9,\Delta_{1,0}=1,\Delta_{2,0}=4)||p^{\text{theo},2}(\mathbf{x}|\gamma_1,\Delta_{1,1},\Delta_{2,1}=4)) = 1.38\cdot 10^{-5},$$

$$\min_{(\gamma_1,\Delta_{1,1})\in\mathbb{R}^+\times\mathbb{R}^+} \log\left(\frac{p^{\text{theo},2}(\mathbf{x}|\gamma_0=0.9,\Delta_{1,0}=1,\Delta_{2,0}=4)}{p^{\text{theo},2}(\mathbf{x}|\gamma_1,\Delta_{1,1},\Delta_{2,1}=4)}\right) = 0.$$

Similarly to the previous scenario, the results for $D(p^{\text{emp}}||p^{\text{theo}})$ depend on the particular sample ($n = 10^6$), but for different samples the obtained results are in the same order of magnitude. These results show that the proposed measures are able to distinguish between very similar operator chains; specifically, the proposed measures prove to be useful tools for determining the ordering of operators in complex chains.

6 Conclusions and future work

This work uses two measures, coming from detection and information theory, for analyzing the distinguishability of different operator parameters working on fixed operator chains, as well as for detecting the ordering and topology of similar chains. The reported results are promising, since the methods based on the proposed measures rightly estimated the applied parameters and operator chains. In the future work, special attention will be paid to experiments with real images, as well as to the comparison with existing ad-hoc schemes in the literature.

References

1. Bianchi, T., Piva, A.: Analysis of non-aligned double JPEG artifacts for the localization of image forgeries. In: Proc. of the IEEE WIFS. Iguacu Falls, Brasil (December 2011)
2. Cachin, C.: An information-theoretic model for steganography. In: Aucsmith, D. (ed.) Information Hiding International Workshop. Lecture Notes in Computer Science, vol. 1525, pp. 306–318. Springer, Portland, OR, USA (April 1998)
3. Comesaña, P., Pérez-González, F.: Detection and information theoretic measures for quantifying the distingsuishability between multimedia operator chains (2012), submitted to IEEE WIFS 2012
4. Cover, T.M., Thomas, J.A.: Elements of Information Theory. Wiley (2006)
5. Fan, Z., de Queiroz, R.L.: Identification of bitmap compression history: JPEG detection and quantizer estimation. IEEE Transactions on Image Processing 12(2), 230–235 (February 2003)
6. Fu, D., Shi, Y.Q., Su, W.: A generalized Benford's law for JPEG coefficients and its applications in image forensics. In: Proc. SPIE 6505. vol. 6505, p. 65051L. San Jose, CA (January 2007)
7. Lin, W.S., Tjoa, S.K., Zhao, H.V., Liu, K.J.R.: Digital image source coder forensics via intrinsic fingerprints. IEEE Transactions on Informations Forensics and Security 4(3), 460 (September 2009)
8. Lukas, J., Fridrich, J.: Estimation of primary quantization matrix in double compressed JPEG images. In: Proc. of DFRWS (2003)
9. Luo, W., Qu, Z., Huang, J., Qiu, G.: A novel method for detecting cropped and recompressed image block. In: Proc. of the IEEE ICASSP. pp. 217–220. Honolulu, HI (April 2007)
10. Luo, W., Wang, Y., Huang, J.: Detection of quantization artifacts and its applications to transform encoder identification. IEEE Transactions on Information Forensics and Security 5(4), 810–815 (December 2010)
11. Milani, S., Tagliasacchi, M., Tubaro, S.: Discriminating multiple JPEG compression using first digit features. In: Proc. of the IEEE ICASSP. Kyoto, Japan (March 2012)